4 August 1994

PHYSICS LETTERS B

ELSEVIER

Physics Letters B 333 (1994) 519–525

Scaling behaviour of jet shapes in $p\bar{p}$ and ep collisions

G. Kramer, S.G. Salesch

II. Institut für Theoretische Physik, Universität Hamburg, Luruper Chaussee 149, D - 22761 Hamburg, Germany[1]

Received 20 April 1994; revised manuscript received 7 June 1994
Editor: P.V. Landshoff

Abstract

We have calculated jet shapes in resolved γp and $p\bar{p}$ collisions in perturbation theory at order α_s^3 for the hard parton-parton processes. We compared the jet shapes for different c.m. energies $\sqrt{S}$ and between the two processes for fixed $x_T = 2E_T/\sqrt{S}$ and fixed cone parameters. We found a simple scaling behaviour of the jet shape which allows its comparison for different reactions and c.m. energies.

1. Introduction

A large fraction of the final state in hadron-hadron, electron-hadron and electron-positron collisions consists of high energy jets. These jets have an extended structure in phase space which can be studied experimentally and theoretically. One possible measure of such jet structure is the so-called jet shape or jet profile which depends on variables like transverse energy and rapidity of the jets, the jet algorithm and the extension of jets.

Some months ago we presented results for jet shapes in resolved γp collisions based on perturbation theory at order α_s^3 for the hard parton-parton scattering processes [1,2]. We studied the jet shape concerning its dependence on transverse energy, rapidity and the inner cone extension. These functional dependencies came out quite similar to those found earlier for $p\bar{p}$ processes at $\sqrt{S} = 1.8$ TeV by Ellis, Kunszt and Soper [3]. We studied this similarity of jet shapes in $p\bar{p}$ and resolved γp collisions further and found interesting scaling properties which allow a direct comparison of jet shapes in these two reactions or in one of these processes for different center of mass energies. The $p\bar{p}$ results are generated with the same program. We just replaced the electron, resp. photon structure function by the parton distributions of the antiproton with the appropriate changes in the hard scattering processes.

The measure of the jet profile is the function $\rho(r, R, E_T, \eta)$ where E_T is the transverse energy of the jet and η is its rapidity with ϕ, its azimuth, integrated out. This function ρ measures the fractional E_T profile, i.e., given a jet sample with transverse energy E_T defined with a cone radius R, then $\rho(r, R, E_T, \eta)$ is the average fraction of the jets' transverse energy that lies inside an inner cone with radius $r < R$. Then the quantity $1 - \rho(r, R, E_T, \eta)$ stands for the fraction of E_T that lies in the cone segment between r and R. This quantity is easily calculated from the contributing $2 \to 3$ parton subprocesses in $p\bar{p}$ or in resolved γp collisions as for $r > 0$ it avoids the collinear singularities at $r = 0$. Therefor it can be computed in a

[1] Supported by Bundesministerium für Forschung und Technologie, 056HH93P(5), Bonn, Germany and EEC Program "Human Capital and Mobility" Network "Physics at High Energy Colliders", CHRX-CT93-0357 (DG12 COMA).

SSDI 0370-2693(94)00785-6

straightforward way from the E_T weighted integral of the $p\bar{p} \to 3$ partons $+ X$ or $\gamma p \to 3$ partons $+ X$ cross sections, respectively, over the cone segment between r and R normalized to $E_{T,J}$ (which is the E_T of the jet) times the Born cross section. This $1 - \rho$ being a ratio of cross sections is $O(\alpha_s)$, since the numerator is proportional to α_s^3, whereas the denominator is $O(\alpha_s^2)$. In the following we shall consider the E_T profile $\rho(r, R, E_T, \eta)$ for γp and $p\bar{p}$ reactions with varying c.m. energies $\sqrt{S}$. In the γp process actually our calculations are for ep scattering where the photon spectrum is obtained in the Weizsäcker-Williams approximation as used in our earlier work [1].

2. Scaling Behaviour of E_T Profile

As explained in the introduction the E_T profile $\rho(r, R, E_T, \eta)$ has the following form

$$\rho(r, R, E_T, \eta) = 1 - \alpha_s(\mu) f(r, R, E_T, \eta) + O(\alpha_s^2) \tag{1}$$

where μ is the scale of the QCD coupling. We take α_s in one-loop approximation with $\Lambda = 194$ MeV, i.e. equal to the Λ value of the chosen protron structure function MT-B1 [4]. $\mu = M_{\gamma,p} = E_T$ where $M_{\gamma,p}$ is the factorization scale of the photon and the proton (antiproton) structure function, respectively. For the γp case the photon structure function is taken from the work of Glück, Reya and Vogt [5] in NLO and $\overline{\text{MS}}$ factorization. Since ρ is a ratio of cross sections the exact form of the structure functions is not really important. Sometimes α_s in two-loop approximation is preferred [3]. This is essentially equivalent to a change of the scale μ or of the value for Λ.

Now we ask, how the function $f(r, R, E_T, \eta)$ defined in (1) behaves when different c.m. energies $\sqrt{S}$ are employed for ep and $p\bar{p}$ processes. As we explained in the introduction $f(r, R, E_T, \eta)$ is given as a ratio of cross sections with an additional factor E_T in the numerator and in the denominator. Therefore f is dimensionless. The E_T dependence in f enters through the structure functions via the scale choice $M \propto E_T$ and through the E_T dependence of the $2 \to 3$ parton-parton scattering cross sections in the numerator and the $2 \to 2$ parton-parton scattering cross section in the denominator. We expect the E_T dependence through the parton distributions being cancelled in the ratio. This has been checked by direct computation [2]. The parton-parton scattering cross sections depend only on dimensionless variables $x_T = 2E_T/\sqrt{S}$, η and the momentum fractions $x_{a,b}$ of the incoming partons apart from a dimensional factor that cancels in the ratio. From these arguments we expect that for fixed η, r, R the function $f(r, R, E_T, \eta)$ depends only on x_T. Therefore f should not depend on the c.m. energy $\sqrt{S}$ when x_T is held fixed. We tested this by calculating $f(r, R, E_T, \eta)$ for various values of r between 0.1 and 0.95, for $x_T = 0.1$ and 0.5, respectively, and $\eta_S = 0$, where η_S is the rapidity in the c.m. system of the ingoing hadrons or electrons. The chosen jet sample has $R = 1$. We considered the following four cases, the two ep processes (resolved photoproduction only) with $\sqrt{S} = 314$ GeV (HERA c.m. energy) and $\sqrt{S} = 1.8$ TeV (TEVATRON c.m. energy, which perhaps could be measured with LEP-LHC) and the two $p\bar{p}$ processes for the same c.m. energies $\sqrt{S} = 314$ GeV and $\sqrt{S} = 1.8$ TeV, respectively. The results are collected in Table 1. We see from these results that the $f(r, R, E_T, \eta)$ for fixed r and x_T are almost identical although $\sqrt{S}$ changes by the factor 5.7, if we compare the results for $p\bar{p}$ and γp separately. The differences between column 2 and column 4 ($x_T = 0.1$) and between column 3 and 5 ($x_T = 0.5$) in the table are on the percent level. The same is true if we compare the columns with the results for the $p\bar{p}$ case. If we compare the f's for $p\bar{p}$ and ep reactions, keeping r and x_T fixed, we find again that the results are very similar, in particular for $x_T = 0.1$ and less for $x_T = 0.5$. This is easy to understand. We see the influence of the point-like component of the photon structure function coming in at large E_T, i.e. at $x_T = 0.5$, which corresponds to $E_T = 79$ GeV and $E_T = 450$ GeV for the low and high c.m. energy, respectively. This difference is expected to be even larger if we had taken into account also the contribution of the direct photon [6]. But at $x_T = 0.1$, i.e. $E_T = 16$ GeV and $E_T = 90$ GeV respectively, the corresponding values for f differ by less than a few percent. This result is remarkable since even for small x_T we expect some difference between the photon and the antiproton structure functions and also the superposition of the various parton-parton scattering cross sections is certainly different in ep and $p\bar{p}$ reactions. It appears that, since f is calculated from a ratio of cross sections, these differences largely cancel. This

Table 1
Comparison of jet profiles for ep and $p\bar{p}$ scattering in terms of $f(r, R, E_T, \eta)$ defined in (1) for $R = 1$, $\eta_S = 0$, c.m. energies $\sqrt{S} = 314$ GeV (HERA) and $\sqrt{S} = 1.8$ TeV (TEVATRON), $x_T = 0.1$ and 0.5 and various r

r	$f(R;r)$							
	ep [HERA]		ep [$\sqrt{S}$ = 1800 GeV]		$p\bar{p}$ [$\sqrt{S}$ = 314 GeV]		$p\bar{p}$ [TEVATRON]	
	$x_T = 0.1$	$x_T = 0.5$	$x_T = 0.1$	$x_T = 0.5$	$x_T = 0.1$	$x_T = 0.5$	$x_T = 0.1$	$x_T = 0.5$
0.95	0.142	0.151	0.147	0.154	0.148	0.191	0.146	0.193
0.9	0.286	0.295	0.285	0.298	0.300	0.373	0.296	0.381
0.8	0.583	0.573	0.586	0.596	0.606	0.713	0.602	0.729
0.7	0.909	0.860	0.912	0.884	0.927	1.05	0.920	1.06
0.6	1.25	1.15	1.25	1.18	1.28	1.37	1.28	1.38
0.5	1.66	1.50	1.68	1.53	1.70	1.74	1.69	1.74
0.4	2.13	1.88	2.15	1.92	2.21	2.10	2.19	2.14
0.3	2.74	2.36	2.75	2.38	2.88	2.62	2.87	2.63
0.2	3.75	3.09	3.76	3.13	3.91	3.40	3.85	3.40
0.1	5.72	4.54	5.77	4.58	6.02	4.85	5.91	4.82

means that the whole E_T dependence of the jet profile $1 - \rho$ originates from the fact that the coupling α_s depends on E_T. So, for example for $x_T = 0.1$ the jets at $\sqrt{S} = 1.8$ TeV are in average narrower by the factor $\alpha_s(E_T = 90\ \text{GeV})/\alpha_s(E_T = 16\ \text{GeV}) \simeq 0.7$ than at $\sqrt{S} = 0.314$ TeV (α_s is calculated in one-loop with $\Lambda = 194$ MeV and four flavours). Therefore, since the variation of α_s with E_T is essentially known, it is possible to predict the E_T profile for any c.m. energy as long it has been measured for one energy. As we have seen this remains true even when we consider different processes as for example $p\bar{p}$ or ep reactions as long as x_T is small ($x_T \simeq 0.1$). In case the fractional E_T profile would be measured for several c.m. energies, say, between 300 and 1800 GeV, the running of α_s with E_T could be studied in detail. Of course with data from LHC this would be possible even more.

That the jet profile $1 - \rho$ is determined from a ratio of cross sections seems to be essential for the close similarity of $\rho(r)$ at small x_T for different reactions. For cross sections we do not expect this. This is demonstrated in Fig. 1 where we compare the single-jet inclusive cross section $d^2\sigma/dE_T d\eta$ for ep scattering and $p\bar{p}$ scattering. For these cross sections we have chosen in both cases $\sqrt{S} = 298$ GeV in accordance with present HERA conditions with c.m. rapidity $\eta_S = 0$. From this comparison it is easily seen that the E_T distributions (at $E_T = 5$ GeV they are normalized to each other by dividing the $p\bar{p}$ cross section by 4000) differ appreciably for $E_T > 20$ GeV. The $p\bar{p}$ cross section is steeper as a function of E_T than the ep cross section at the same c.m. energy. The curves in Fig. 1 are in LO and in NLO with $R = 1$. The less steep behaviour of the ep cross section, of course,

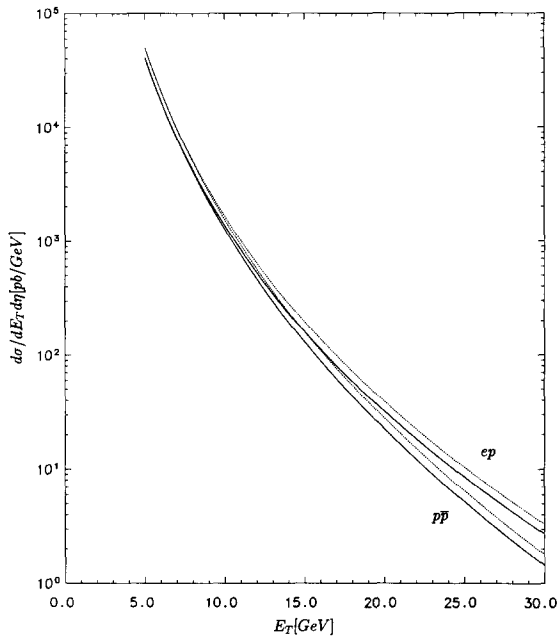

Fig. 1. Inclusive single-jet cross section in leading order (full) and in next-to-leading order (dotted) with $R = 1$ and $\eta_S = 0$. Shown are the cross sections for electroproduction (upper lines) and for $p\bar{p}$ scattering (lower lines) divided by 4000 both for $\sqrt{S} = 298$ GeV.

originates from the point-like or anomalous part of the quark distribution function of the photon. This effect is even more drastic at larger E_T when the contribution for direct photoproduction is added [7].

So far we considered the function $f(r, R, E_T, \eta)$ defined in (1) for fixed rapidity η only. Above we saw that f does not change with $\sqrt{S}$ when considered as a function of x_T. This will be true for all η although in the table we presented evidence only for $\eta_S = 0$. It is clear that f considered as a function of r, R, x_T and η will vary differently with η depending on the value of x_T since the phase space limits on η are $\eta \leq \operatorname{arcosh}(x_T^{-1})$. In [1] we computed the profile function $\rho(r, R, E_T, \eta)$ for $r = 0.3$ as a function of η and for $E_T = 5$, 15 and 30 GeV for γp collisions with $\sqrt{S} = 314$ GeV. The curves in Fig. 3 of [1] are rather alike in shape except for the different phase space limits in η which change with x_T. This suggest that we introduce instead of η the scaled rapidity

$$x_\eta = \frac{\eta_S}{\operatorname{arcosh}(x_T^{-1})} \tag{2}$$

so that $|x_\eta| \leq 1$ and try the following scaling ansatz for ρ:

$$\rho(r, R, E_T, \eta) = 1 - \alpha_s(\mu) f_1(r, R, x_T) f_2(r, R, x_\eta) \tag{3}$$

so that the x_T and the x_η dependence factorize. In Figs. 2a,b we have plotted $f_2(r, R, x_\eta)$ for two cases: (a) $p\bar{p}$ reaction and $\sqrt{S} = 1.8$ TeV and (b) ep reaction and $\sqrt{S} = 0.314$ TeV where the curves in Figs. 2a,b are calculated with $r = 0.3$, $R = 1$ and are for $x_T = 0.035$, 0.1, 0.2, respectively. We see that all curves are rather universal, i.e. independent of x_T, so that the factorization hypothesis in (3) is approximately fulfilled. The factorization in (2) is defined up to a x_η independent factor. The functions in Figs. 2a,b are normalized, so that

$$f_1(r, R, x_T) = f(r, R, E_T, \eta_S = 0) \tag{4}$$

and

$$f_2(r, R, x_\eta) = \frac{f(r, R, E_T, \eta_S)}{f(r, R, E_T, \eta_S = 0)} \tag{5}$$

or

$$f_2(r, R, x_\eta) = \frac{1 - \rho(r, R, E_T, \eta_S)}{1 - \rho(r, R, E_T, \eta_S = 0)} \tag{6}$$

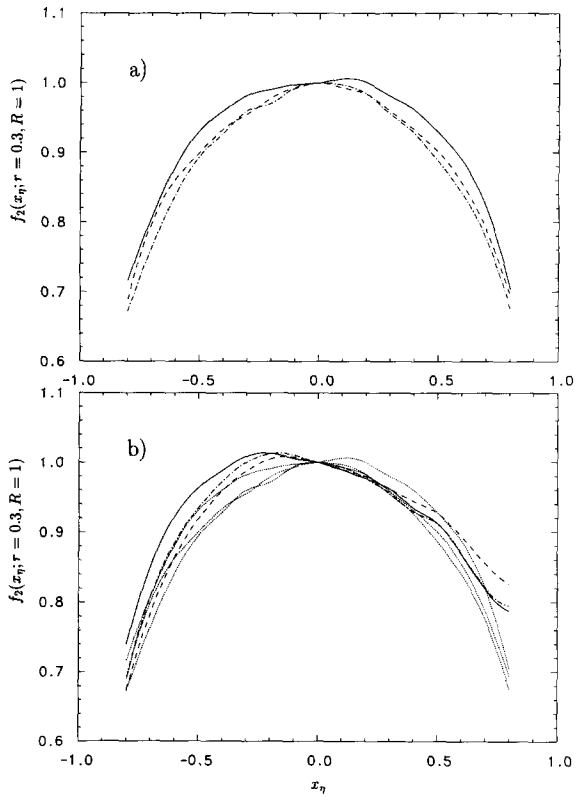

Fig. 2. f_2 as defined by (5) as a function of x_η (see (2)) for $R = 1$, $r = 0.3$ and different values of $x_T = 0.035$ (full), 0.1 (dashed) and 0.2 (dash- dotted) for a) $p\bar{p}$ scattering at $\sqrt{S} = 1.8$ TeV and b) ep scattering at $\sqrt{S} = 314$ GeV. The dotted curves are the curves of a).

making (3) consistent with (1). In Fig. 2b we have included also the three $p\bar{p}$ curves (dotted) for comparison with the ep results. It turns out that f_2 depends only weakly on r. We observe in Fig. 2a that the $p\bar{p}$ process is rather symmetric in x_η ($x_\eta > 0$ is the direction of the incoming antiprotron) independent of x_T. For ep scattering the curves are not symmetric in x_η since the parton distributions of the photon and the proton are different. In addition we observe in this case that the maximum of f_2 is at negative x_η for small x_T and is shifted to positive x_η if x_T increases. This can be understood by studying the contributing parton-parton scattering processes. So the shift of the maximum is caused by the $q_\gamma^{an} g_p$ scattering process where q_γ^{an} stands for the contribution of the point-like part of the photon structure function and g_p for the gluon induced part of the proton structure function.

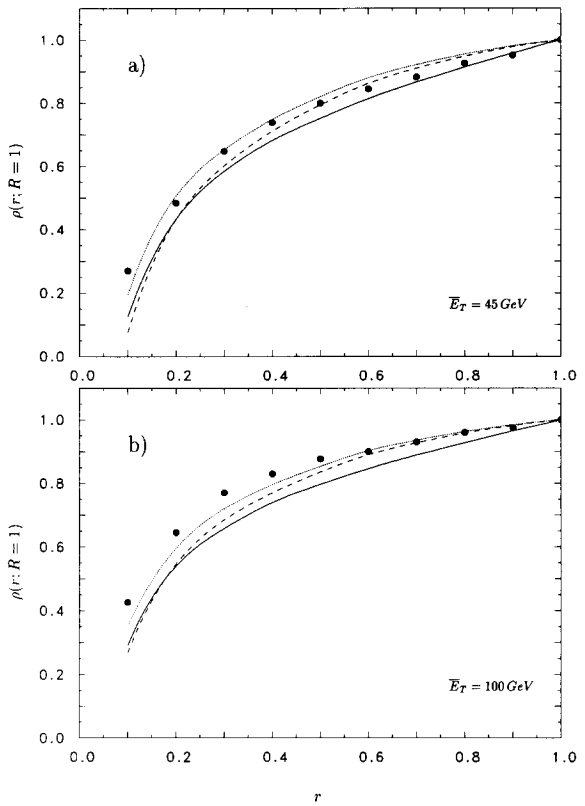

Fig. 3. The relative E_T profile ρ versus r for $R = 1$ and $0.1 \leq |\eta| \leq 0.7$. The CDF data (full circles) are compared with theoretical results for different combinations of $(\mu/E_T, R_{sep}/R) = (1,2)$ [full], $(1,1.5)$ [dotted] and $(0.5,1.5)$ [dashed] at a) $\overline{E_T} = 45$ GeV, b) $\overline{E_T} = 100$ GeV.

At small x_T the $g_\gamma\, g_p$ parton-parton scattering process with the corresponding structure functions dominates.

So far experimental data have been published only for $p\bar{p}$ reactions [8–10]. Preliminary data from the ZEUS collaboration at HERA exist and better data are expected soon [11]. In Fig. 3 we show the comparison of $\rho(r)$ with data from CDF [9]. In this plot the data are taken for $R = 1$, $0.1 \leq |\eta| \leq 0.7$ and $\overline{E_T} = 45, 100$ GeV i.e. the E_T are in the ranges 40–60 and 95–120 GeV. For both E_T ranges we have calculated three curves (with the same averaging over E_T and η as for the data), two with renormalization scale $\mu = E_T$, but different separation cone R_{sep} and one with scale $\mu = E_T/2$. The curves with $\mu = E_T$ and $R_{sep} = 1.5\,R$ instead of $R_{sep} = 2\,R$, which is the canonical value without overlap corrections, give the best fit. The parameter R_{sep} accounts for the problem of jet separation. In the theory two partons are separated if they are more distant than $2\,R$. Experimentally, however, it may happen that the tails of two jets overlap and that the separation between the jet cones is less than $2\,R$. Thus following [3] we inserted a new parameter in the theoretical calculation: R_{sep} which is the minimum separation between two jets. By comparing with CDF data a value of $R_{sep} = 1.3$ was found adequate [3]. (Further details for the justification of R_{sep} are found in [3]). We see that the decrease of R_{sep} as compared to the canonical value influences the behaviour of ρ for the r values near the boundary $r = R$ whereas the change of the scale parameter influences $\rho(r)$ for the smaller r values, larger $\mu's$ lead to an increase of ρ. For very small r we have the influence of higher order corrections so that we can not expect a good fit anymore. For $\overline{E_T} = 45$ GeV the fit is better for small r than for large r, whereas for $\overline{E_T} = 100$ GeV it is the opposite. So at $\overline{E_T} = 45$ GeV we would expect a different combination of μ and R_{sep} to give a "best fit" to the data. In general, looking at ρ as a function of E_T (or better x_T) while keeping r fixed would require E_T dependent μ, R_{sep} pairs. This can be seen more directly by comparing with the data of the UA1 collaboration who has measured the dependence of ρ on E_T at $r = 0.2$. These data show a strong decrease of $\rho(E_T)$ when E_T is below 40 GeV ($x_T \leq 0.12$), which can not be explained theoretically with fixed μ/E_T and R_{sep}. We attribute this partly to the small r value where higher order effects and fragmentation corrections are much more important. The D0 data [10] are very similar to the CDF data and therefore have not been used for comparison with theory. As compared to earlier work [3] who obtained similar results we remark that they used the two-loop formula for α_s and different structure functions. In particular the formula assumed for α_s influences the $\rho(r)$ at smaller r's. We reproduced their results with our program when we use their input concerning α_s and the proton structure function, so obtaining an independent check of the results in Ref. [3].

In order to demonstrate that the scaling behaviour (1) for the jet shape $\rho(r)$ is useful we have taken the data for $\rho(r)$ as measured by CDF in $p\bar{p}$ collisions and compared in Fig. 3 with our calculations and have converted them on the basis of (1) into a prediction of $\rho(r)$ for ep collisions at the HERA energy $\sqrt{S} =$ 314 GeV. We have done this for the data at $\overline{E_T} =$

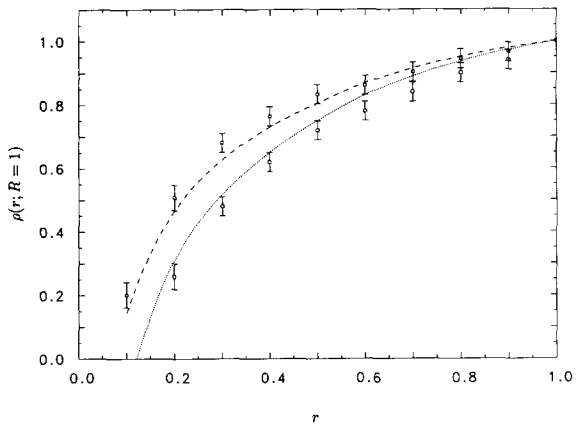

Fig. 4. The relative E_T profile ρ versus r for $R = 1$, $R_{sep} = 1.5$, $0.1 \leq |\eta| \leq 0.7$, $\overline{E_T} = 7.85$ GeV (dotted) and $\overline{E_T} = 17.4$ GeV (dashed) compared to ρ's obtained from CDF data with the help of the scaling law (1). Open circles for $\overline{E_T} = 7.85$ GeV, open squares for $\overline{E_T} = 17.4$ GeV.

45 GeV and 100 GeV. For fixed x_T this translates into $\overline{E_T} = 7.85$ GeV and 17.4 GeV at HERA. The averaging in E_T in the ranges 40–60 and 95–120 GeV goes over into the ranges 6.98–10.4 and 16.6–20.9 GeV, respectively. The CDF data were also averaged over η in the interval $0.1 \leq |\eta| \leq 0.7$. This averaging over η is not essential since f does not change for fixed η. In addition in the central region f is nearly independent of η [1]. The same range of η applies also to the results of the conversion at $\sqrt{S} = 314$ GeV. They are shown as points in Fig. 4. In our comparison in Fig. 3 the choice of $R_{sep} = 1.5$ gave a good fit to the CDF data. Therefore the points in Fig. 4 are also for $R_{sep} = 1.5$ if they should be compared to a theoretical calculation for ep scattering. This we have done for $\sqrt{S} = 314$ GeV and with averaging over the respective E_T and η ranges given above. The results are shown as dashed ($\overline{E_T} = 17.4$ GeV) and as dotted ($\overline{E_T} = 7.85$ GeV) curves. The agreement between the "experimental" points and the curves is satisfactory. This shows that the conversion of the CDF data into ep data works also for $R_{sep} < 2R$ ($R_{sep} = 2R$ was chosen for the comparison in Table 1). Furthermore, the conversion reproduces the correct dependence of $\rho(r, R, E_T, \eta)$ as a function of r and E_T. For fixed r the jets become narrower with increasing E_T. Concerning the quality of agreement between the points and the curves in Fig. 4 we must take into account that the fit of the theory with separation $R_{sep} = 1.5$ to the CDF data was not perfect either. So, for example, the CDF points for $\overline{E_T} = 100$ GeV in Fig. 3b are also slightly above the theoretical curve in the range $r \leq 0.5$. The same occurs in Fig. 4 for the points at $\overline{E_T} = 17.4$ GeV.

3. Conclusions

We have seen that the E_T jet profiles in $p\bar{p}$ and ep collisions are very much alike. If considered as a function of x_T instead of E_T the shape function $(1 - \rho(r, R, x_T, \eta))/\alpha_s$ for different c.m energies $\sqrt{S}$ and different processes are very approximately the same. Thus for $(1 - \rho)$ the remaining S dependence appears only via the scale dependence of $\alpha_s(\mu)$ which is known. This is valid in particular for all x_T when only the jet shapes of one process but for different energies are considered. It is less valid for large x_T if we compare jet shapes in ep and $p\bar{p}$ processes. In this case the effect of the anomalous quark distribution of the photon comes into play. A conversion of CDF data for ρ into jet shapes for ep at HERA gave very encouraging results. This shows that jet shapes in the perturbative regime, i.e. at large angles at the edge of the cone, are rather universal and independent of the c.m. energy if α_s is factored out in $1 - \rho$. Near the jet axis the jet shape is dominated by collinear soft gluon emission. It would be interesting to see how the scaling law valid in the perturbative regime is changed in this region.

Acknowledgement

We wish to thank F. Barreiro and J. Terron for their interest and for fruitful discussions on preliminary data from ZEUS.

References

[1] G. Kramer, S.G. Salesch, Phys. Lett. B 317 (1993) 218.
[2] S.G. Salesch, DESY report 93-196 (December 1993).
[3] S.D. Ellis, Z. Kunszt, D.E. Soper, Phys. Rev. Lett. 69 (1992) 3615.
[4] J.G. Morfin, Wu-Ki Tung, Z. Phys. C 52 (1991) 13.
[5] M. Glück, E. Reya, A. Vogt, Phys. Rev. D 46 (1992) 1973.
[6] D. Bödeker, Phys. Lett. B 292 (1992) 164; Z. Phys. C 59 (1993) 901;
L.E. Gordon, J.K. Storrow, Phys. Lett. B 291 (1992) 320;
M. Greco, A. Vicini, preprint LNF-93/017-P (April 1993).

[7] D. Bödeker, G. Kramer, S.G. Salesch, DESY report 94-042 (March 1994).
[8] UA1 Collaboration, F. Albajar et al., Nucl. Phys. B 309 (1988) 405.
[9] CDF Collaboration, F. Abe et al., Phys. Rev. Lett. 68 (1992) 1104.
[10] D0 Collaboration, G.C. Blazey, talk at the DESY THEORY WORKSHOP, September 1993, entitled QCD Results from $\bar{p}p$ Colliders.
[11] F. Barreiro, J. Terron, private communication.